Turkish Journal of Engineering

Turkish Journal of Engineering (TUJE)
Vol. 3, Issue 2, pp. 68-75, April 2019
ISSN 2587-1366, Turkey
DOI: 10.31127/tuje.453593
Research Article

INVESTIGATION OF OXYGEN-RELATED DEFECTS IN ZnO: GROWING TIME AND Mn CONCENTRATION EFFECTS

Selma Erat[1,2*], Saadet Yıldırımcan[3]

[1]Mersin University, Vocational School of Technical Sciences, Department of Medical Services and Techniques, Program of Opticianry, Mersin, Turkey
[2]Advanced Technology, Research and Application Center, Mersin University, Mersin, Turkey
ORCID ID 0000 – 0001 – 7187 – 7668
selmaerat33@gmail.com

[3]Toros University, Faculty of Engineering, Department of Electrical-Electronics, Mersin, Turkey
ORCID ID 0000 – 0002 – 9044 – 6908
saadetyildirimcan@gmail.com

* Corresponding Author
Received: 14/08/2018 Accepted: 12/09/2018

ABSTRACT
The optical and photoluminescence properties of ZnO nanocrystals synthesized via hydrothermal method are determined in this study. The effect of growing time (1 h, 6 h, 12 h, 24 h and 36 h) and Mn concentration ($5x10^{-4}$ mol, $10x10^{-4}$, $25x10^{-4}$ mol, $75x10^{-4}$ mol, $100x10^{-4}$ mol, $250x10^{-4}$ mol) on these properties are investigated and presented in detail. The ultraviolet–visible (UV-Vis) and photoluminescence (PL) spectroscopy techniques are used for optical and photoluminescence properties characterization. Room temperature PL spectra of the ZnO nanopowders show a near band-edge emission (peak at 385 nm) and a red light emission (peak at 650 nm) for both ZnO synthesized for different growing time and different Mn concentration. The ZnO prepared with 1 h and 12 h includes the lowest oxygen related defects. The ZnO doped with $5x10^{-4}$ mol shows the highest oxygen related defects whereas that of $100x10^{-4}$ mol shows the lowest defects.

Keywords: *ZnO, Mn, Photoluminescence Properties, Optical Properties, Nanoparticles*

1. INTRODUCTION

Zinc oxide (ZnO) being which is an intrinsic n-type II-VI semiconductor and have a wide-band gap (3.37 eV) and a large exciton binding energy (60 meV, at room temperature) has received considerable attention since it is low cost, non-toxic, chemically stable, high thermally stable environmentally friendly and further its optical and electrical properties can be tuned by doping (Putri *et al*., 2018; Karmakar *et al*., 2012; Kadam *et al*., 2017; Dhara *et al*., 2018; Fan *et al*., 2004; Wang *et al*., 2011; Choudhury *et al*., 2016). Therefore, ZnO has several applications such as gas sensors (Wang *et al*., 2017; Wang *et al*., 2015; Othman *et al*., 2017), solar cells (Dhara *et al*., 2018; Sekine *et al*., 2009; Keis *et al*., 2002; Law *et al*., 2005; Martinson *et al*., 2007), and light emitting diodes (Saito *et al*., 2002), optical modulator waveguides (Koch *et al*., 1995), field effect transistor (Vijayalakshmi *et al*., 2015), UV detectors (Das *et al*., 2010), and surface acoustic wave filters (Emanetoglu *et al*., 1999). ZnO has been synthesized using different techniques such as microwave-assisted synthesis (Schneider *et al*., 2010), sol–gel processing (Bahnemann *et al*., 1987), hydrothermal synthesis (Li *et al*., 2001), aerosol spray analysis (Motaung *et al*., 2014), wet chemical (Toloman *et al*., 2013) and hydrolysis/condensation (Cohn *et al*., 2012).

It was reported that doping ZnO with transition metal ions such as Mn, Fe, Co, Ni, and Cu reduced the band gap energy and prevent electron-hole pair recombination through the generation of new states (Achouri *et al*., 2016; Anandan *et al*., 2007; Chauhan *et al*., 2012; Saleh *et al*., 2014; Bhatia *et al*., 2017; Nasser *et al*., 2017; Tabib *et al*., 2017; Altintas Yildirim *et al*., 2016). Besides, it is known that tuning the morphology of ZnO nanostructure turns out variations in optical and electrical properties (Awad *et al*., 2015). Among all of the aforementioned transition elements, the most encouraging one is Mn for doping ZnO nanostructure because Mn with valence state of 2+ has the highest possible magnetic moment (Khanna *et al*., 2003). Further, substituting Mn ions into ZnO may enhance the photocatalytic activity under UV and visible irradiation and that is attributed to an increase in the number of defect sites acting as electron traps that effectively suppresses the recombination of the photogenerated carriers (Achouri *et al*., 2016; Saleh *et al*., 2014; Ma *et al*., 2016; Barzgari *et al*., 2016; Umar *et al*., 2015; Donkova *et al*., 2010; Ullah *et al*., 2008).

There are some other studies about Mn doped ZnO for instance Deka *et al*. (Deka *et al*., 2007) reported that doping Mn ions in ZnO results in an increase in both of unit cell volume and the optical band gap. In addition, Li et al. (Moontragoon *et al*., 2013) demonstrated that Mn doped ZnO nanorods had a strong near band-edge emission and a weak deep level emission. It was an aim of our group to investigate the changes of local environment of doped ion Mn^{2+} in ZnO (Yildirimcan *et al*., 2016). The defects in pure ZnO and Mn doped Mn were determined via electron paramagnetic resonance (EPR) and it was concluded that structural defects due to Zn and O vacancies were dominant compared to extrinsic (Mn^{2+} ion) structural defects (Yildirimcan *et al*., 2016). Since the synthesis process and characterization of the electronic and thermal properties of our ZnO and Mn doped ZnO nanocrystals were studied via x-ray diffraction (XRD), thermogravimetry (TG), differential thermal analysis (DTA), field emission-scanning electron microscopy (FE-SEM), transmission electron microscopy (TEM), energy dispersive x-ray (EDX), inductively coupled plasma mass spectrometry (ICP-MS) techniques by our group (Yildirimcan *et al*., 2016), here in this study we focus on the optical properties of those samples of ZnO and Mn doped ZnO nanocrystals synthesized by using hydrothermal route. The ultraviolet–visible (UV-Vis) and photoluminescence (PL) spectroscopy techniques are used in order to investigate the optical properties of the samples.

2. EXPERIMENTAL PROCESS

The ZnO and Mn-doped ZnO nanopowder was synthesized with the hydrothermal technique in Teflon-lined autoclave at 70 °C. The synthesis of these samples is the same as our previously published study (Yildirimcan *et al*., 2016). The precursor solutions were prepared using the stoichiometric amount of zinc nitrate hexahydrate ($Zn(NO_3)_2$ $6H_2O$, Acros Organics), polyethylene glycol (PEG300, Aldrich Chemistry) and ammonia (NH_3, Analar Normapur) to produce ZnO nanopowders. ZnO nanopowders were synthesized for various duration times such as 1 h, 6 h, 12 h, 24 h and 36 h. The $Mn(NO_3)_2$ $4H_2O$ solution was prepared certain Mn^{2+} concentration (X1: undoped, X2: 5 $x10^{-4}$ mol; X3: 10 x 10^{-4} mol; X4: 25 x 10^{-4} mol; X5: 75 x 10^{-4} mol; X6: 100 x 10^{-4} mol; X7: 250 x 10^{-4} mol). These solutions were added into the solutions, which are used to prepare ZnO nanopowders (6 h) and the synthesis of Mn doped ZnO nanopowders was performed. Finally, the precipitation of ZnO and ZnO:Mn was filtered, washed with distilled water, and were dried in an oven at 80 °C for 1 h (Yildirimcan et al., 2016). All of the details about the chemical reaction mechanisms followed for the formation of ZnO and Mn doped ZnO were given (Yildirimcan *et al*., 2016).

Photoluminescence (PL) measurements of the nanocrystals were made by using a Varian Cary Eclipse Fluorescence spectrophotometer. The UV-visible spectra of the nanocrystals were recorded by using UV-1800 Shimadzu UV-Vis spectrophotometer in the range 200-900 nm.

3. RESULTS AND DISCUSSIONS

Recently, the crystallographic structure of the ZnO and Mn doped ZnO was presented by our group (Yildirimcan *et al*., 2016) and is summarized in this study for the reader to get a view of all properties. The crystallographic structures of the nanocrystals were defined in following:

The samples synthesized for 1 h, 6 h, 12 h, 24 h, and 36 h were grown in hexagonal wurtzite structure, which was well coincided with JCPDS no: 36-1451. The (101) direction was preferred by the samples synthesized for 1 h-24 h whereas (002) was preferred by the sample 36 h. It was calculated that the crystallite sizes of the samples are increased from 30 nm to 51 nm upon growing time increase from 1 h to 36 h. On the other hand, Mn doped ZnO samples (X2-X7) were formed in hexagonal structure, which was well coincided with JCPDS no: 03-0888. There were no observed systematic increases of

crystallite size by increasing the Mn concentration in ZnO. Fig. 1 shows the change in the lattice parameter of for the samples synthesized for 1 h − 36 h and synthesized with different Mn concentration (Yildirimcan *et al*., 2016).

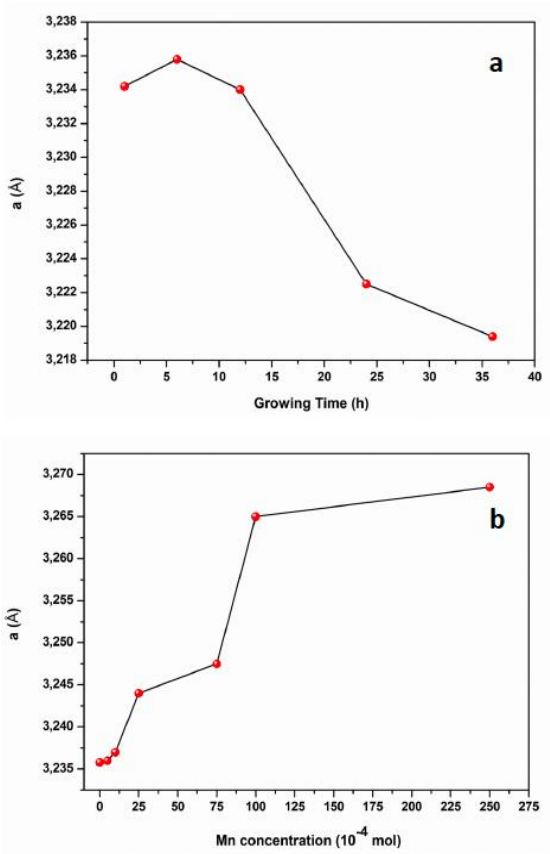

Fig. 1. Change in the lattice parameter of a in hexagonal structure of ZnO (a) depending growing time (b) depending on Mn concentration (Yildirimcan *et al*., 2016)

The highest value of *a* is observed for the sample prepared for 6 h in the series presented in Fig. 1 (a). Besides, the value of *a* is increased upon Mn concentration increase as it is shown in Fig. 1 (b).

Photoluminescence and optical properties, which are the main scope of this study, are investigated and presented in detail. The results were presented in two different sections in following. The comparisons of the results with literature are presented in the discussions part.

3.1. Photoluminescence Analysis of ZnO nanoparticles: Growing Time and Mn Concentration Effects

Photoluminescence (PL) spectra are recorded by using a Varian Cary Eclipse Fluorescence spectrophotometer. The PL measurements of ZnO synthesized with different growing time and Mn doped ZnO nanoparticles were performed under the excitation wavelength of λ_{ex}: 325 nm. Fig. 2 shows the PL spectra of ZnO nanocrystals synthesized for different growing time.

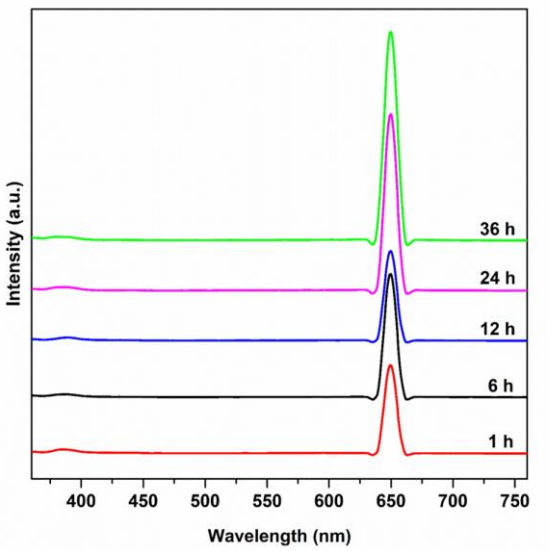

Fig. 2. PL spectra of ZnO synthesized for different growing time.

As it is easy to observe in Fig. 2, there is a significant change in the peak exists at around 650 nm. However, it is difficult to observe the change in peak at around 390 nm. Therefore, Fig. 3 shows the change in PL spectra of ZnO depending on growing time (a) UV emission peak in the wavelength 370-410 nm and (b) red emission peak in the wavelength 640-660 nm.

The wavelengths of UV emission of ZnO nanopowders prepared for 1 h, 6 h, 12 h, 24 h and 36 h are 386 nm (3.22 eV), 387 nm (3.21 eV), 389 nm (3.19 eV), 384 nm (3.23 eV) and 383.5 nm (3.24 eV), respectively.

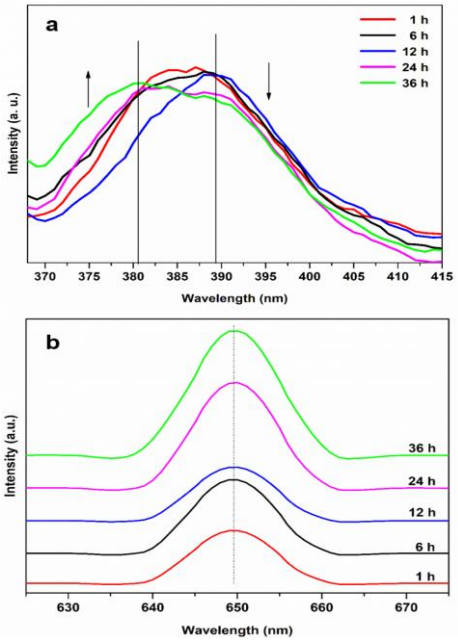

Fig. 3. Enlarged (a) UV peak and (b) visible light emission of ZnO nanoparticles depending on growing time.

The UV peak is characteristic emission peak of ZnO, which is a near band-edge emission. Also, ZnO has very

good UV emission characteristics. (Wei *et al*., 2010). There was no significant change in the UV peak intensity of ZnO nanopowders depending on the growing time. The samples prepared for 6 h and 12 h shift to a longer wavelength, while those prepared for 24 h and 36 h shift to a shorter wavelength.

The red emission peaks of ZnO prepared for different growing times are shown in Fig. 3 (b). The peaks exist at around the wavelength of 650 nm. The change in the PL spectra of ZnO depending Mn concentration is shown in Fig. 4.

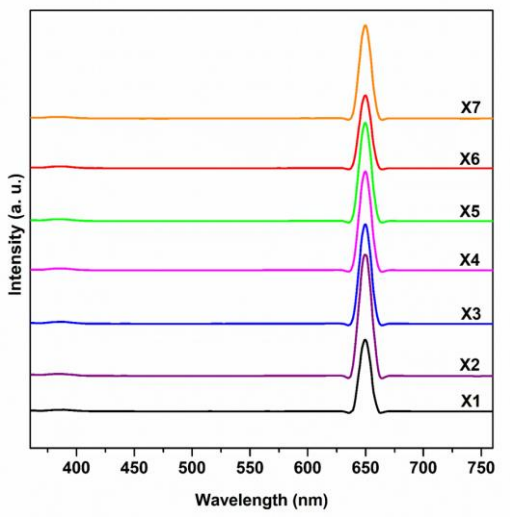

Fig. 4. PL spectra of ZnO:Mn nanoparticles.

Since it is difficult to follow the change both in UV peak and red emission peak in this figure, the peaks are redrawn separately in Fig. 5 (a) and (b), respectively. The UV emission wavelength of Mn doped ZnO nanopowders is 386 nm, 384.23 nm, 386.15 nm, 385.6 nm, 384.7 nm, 386 nm and 382.65 nm for X1 (undoped), X2, X3, X4, X5, X6, and X7, respectively.

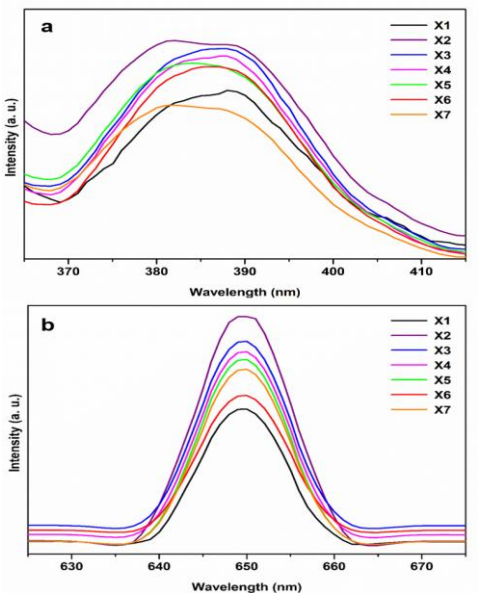

Fig. 5. Enlarged (a) UV peak and (b) visible light emission of ZnO nanoparticles depending on Mn concentration.

It is difficult to observe a systematic change neither in peak position nor in intensity of the UV peak upon Mn concentration increase. It was not observed a regular change in the UV peak wavelength and intensity of Mn doped ZnO nanoparticles depending on the Mn^{2+} concentration. In Fig. 5 (b), the red emission peaks are observed at the wavelength of 650 nm for Mn doped ZnO samples in agreement with the literature (Kaftelen *et al*., 2012).

3.2. Optical properties of ZnO nanoparticles: Growing Time and Mn concentration effects

The UV–visible spectra of the nanoparticles were recorded using UV–1800 Shimadzu UV-Vis spectrophotometer in the range 200 – 900 nm at room temperature (RT). Figure 6 shows the RT absorbance spectra of ZnO nanocrystals prepared for different growing time (1 h, 6 h, 12 h, 24 h, and 36 h).

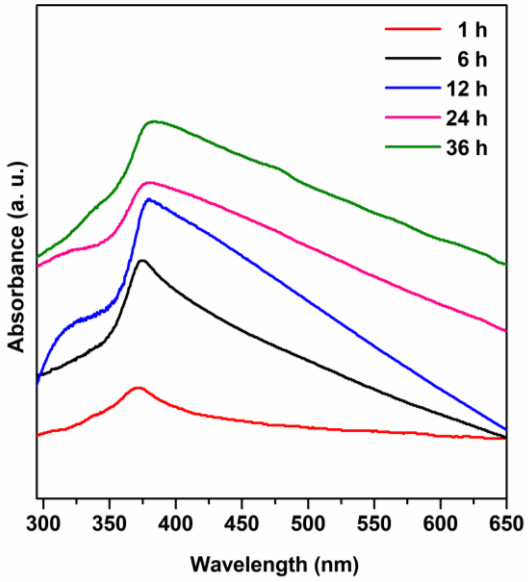

Fig. 6. UV-VIS absorbance spectra of ZnO nanoparticles depending on growing time

The absorbance peaks known as excitonic absorption peaks of the samples appeared in the wavelength range of 350 nm – 420 nm. Namely, the excitonic peak exists at 371 nm, 374 nm, 379 nm, 380 nm, and 382 nm for the sample synthesized for 1 h, 6 h, 12 h, 24 h, and 36 h, respectively. It was mentioned in the literature (Samanta *et al*., 2018) that the absorbance spectra of nanostructures were affected by various factors such as particle size, defect of structure, oxygen vacancy. A small shift toward higher wavelength known as red shift is observed with increasing growing time. The reason for red shift might be increasing concentration of oxygen vacancies on surface ZnO nanopowders (Ahmed, 2017).

Figure 7 shows the change in the excitonic absorption peak position in energy scale (eV) depending on the growing time.

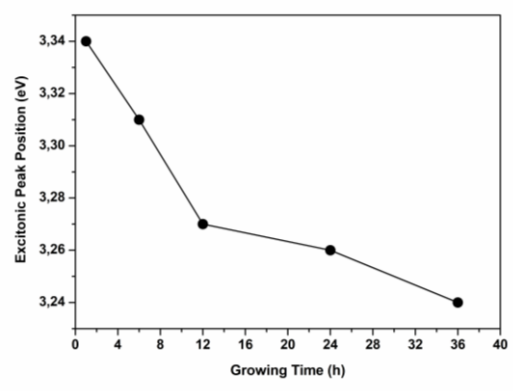

Fig. 7. The change in the excitonic absorption peak position of ZnO depending on growing time

It is observed in Fig. 7 that there is a decrease at the peak position with increasing growing time.

Fig. 8 shows the RT UV–visible absorbance spectra of ZnO nanocrystals doped with different Mn^{2+} concentrations in the wavelength range of 200 nm – 700 nm. It is noticed that the spectra of ZnO is changed drastically once it is doped with Mn^{2+} ions. However, increasing Mn^{2+} ion concentration does not make any change in the spectra significantly. The absorbance peak occurred at 374 nm for undoped ZnO (X1) and 372 nm, 372 nm, 370 nm, 370 nm, 372 nm, 372 nm for X2, X3, X4, X5, X6, and X7, respectively. An extra absorption peak starts to be existed with Mn^{2+} ions doping in ZnO.

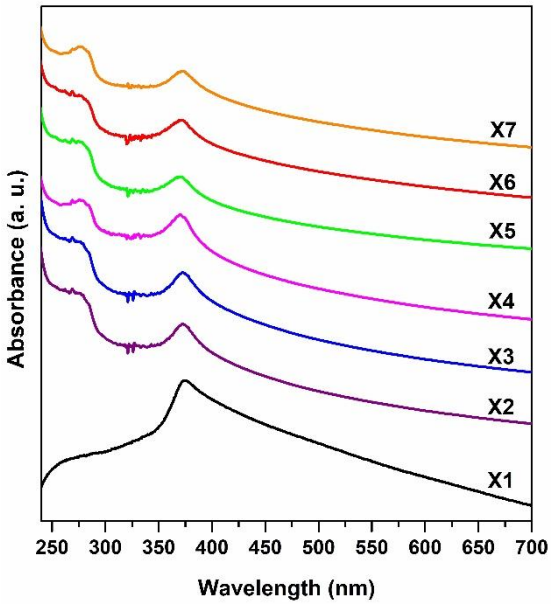

Fig. 8. UV-VIS absorbance spectra of ZnO:Mn nanoparticles depending on Mn concentration

The main part of our discussion is about photoluminescence of the ZnO and ZnO:Mn since there are quite different explanation especially about the origin of visible light emission in PL spectra. It is obvious that the concentration of defects should be reduced in order to fabricate high efficient optoelectronic devices. Thus, firstly it is important to determine the origin of defects created in the structure in other words the origin of defect related emission in visible region. Besides, it is known that different techniques to produce nanomaterials play a role on morphology as well as different types of defects and following different luminescence spectra. Namely, different defects are responsible for the variable visible emissions. For instance, it was reported (Gong et al., 2007) that red emission which takes place in the PL spectra at around (620 nm–780 nm) is originated by mainly either oxygen interstitials or oxygen vacancies. Besides, it was mentioned that oxygen vacancy has three possible charge states in following (Gong *et al*., 2007): the neutral oxygen vacancy (V_O^0), the singly ionized oxygen vacancy ($V_O^{\cdot}$) and the doubly ionized oxygen vacancy ($V_O^{\cdot\cdot}$). Since the single ionized state is thermodynamically unstable with respect to the first principle calculations (Erhart *et al*., 2006; Janotti *et al*., 2005), it is not possible for the oxygen vacancy to be existed in single ionized state. Further, the neutral oxygen vacancies having the lowest formation energy will dominate for ZnO nanoparticles in n-type bulk form. It was observed in the literature that the red-orange emission peak position at ~640–680 nm or ~1.8–1.9 eV was less commonly observed than green and yellow emissions (Studenikin et al., 1998; Mei et al., 2005; Vlasenko *et al*., 2005; Radoi *et al*., 2003; Wu *et al*., 2006; El Hichou *et al*., 2005) and the effect of excitation wavelength on green, yellow, and orange defect emission form ZnO nanostructures (Djurisic *et al*., 2006).

In this study, the PL spectra of ZnO nanocrystals prepared for different growing time and doped with different Mn concentrations are measured at RT. In both of cases, the PL spectra consist of two peaks: first peak is occurred at ~370–400 nm (3.10–3.35 eV) know as typical UV emission peak, which is attributed to band-edge emission or donor-band excitation (Glushenkov *et al*., 2007) and second one at ~640–660 nm (1.87–1.94 eV) visible light emission, red emission. It was reported (Alvi *et al*., 2011) that the red emission of ZnO occurred between 620–750 nm could be attributed to oxygen interstitials (O_i) for the range from 620 nm to 690 nm and to oxygen vacancies (V_o) for the range from 690 nm to 750 nm. The UV peak known as exciton emission shift is due to crystal defects and Burstein-Moss Effect (Chang *et al*., 2012). The long-wavelength shift is related to defects, while short-wavelength shift is related to Burstein Moss effect. That is, the band gap is expanded by the short wavelength shift (Chang *et al*., 2012).

The intensity of the red-light emission at 650 nm increases drastically with increasing growing time except for the sample grown for 12 h. Thus, we can conclude that the 12 h sample has the lowest oxygen related defects in the samples of 6h, 24 h, and 36 h. On the other hand, it is difficult to observe a linear correlation between Mn concentration and so-called red peak emission intensity centered at ~650 nm. In this series, the undoped ZnO shows the lowest intensity and once it is doped $5x10^{-4}$ mole of Mn (X2) shows the strongest intensity. The PL intensity decreases with increasing concentration from $5x10^{-4}$ (X3) to $5x10^{-4}$ (X6) and then the intensity increases for X7.

Wei *et al*., 2010 calculated the intensity ratios of the UV to visible light emission peak as a function of annealing temperature. They concluded that the largest

intensity ratio with the lowest defect emission was obtained by annealing at 700°C. The similar intensity ratios of our PL spectra are calculated and the results shows that the ratios of the samples 1 h and 12 h are very close to each other (0.0305 and 0.0302) and these are the values which are greater than those of the samples 6 h, 24 h, and 36 h (0.0185, 0.0125, and 0.0070). From the point of view of intensity ratio of PL spectra we can conclude that doping ZnO with Mn^{2+} ions creates oxygen related defects in the structure. The sample labeled with X6 shows the lowest oxygen related defects where as that of X2 shows the highest defects.

4. CONCLUSIONS

In the present work, the effects of growing time and Mn concentration on the photoluminescence and optical properties of ZnO nanocrystals synthesized by hydrothermal method have been investigated. It is concluded that the sample prepared for 36 h has the highest oxygen related defects whereas 1 h and 12 h samples have the lowest defects. Besides, doping Mn^{2+} ions creates similar defects in ZnO. However, there is no linear correlation observed between Mn^{2+} concentration and the defect concentration. While the sample X2 also has the highest oxygen related defects, the sample X6 has the lowest defects. We conclude that all of these oxygen related defects are originated by either oxygen interstitial or oxygen vacancies. In addition, these oxygen vacancies should be neutral oxygen vacancies and not by single ionized or doubly ionized oxygen vacancies existing in the structure. In the UV–visible spectra of ZnO the red shift is observed with increasing growing time. Doping Mn^{2+} ions in ZnO creates an extra peak at around 279 nm. However, increasing Mn^{2+} concentration does not change the UV-visible spectra significantly in ZnO:Mn samples.

REFERENCES

Achouri, F., Corbel, S., Balan, L., Mozet, K., Girot, E., Medjahdi, G., Ben, M., Ghrabi, A. and Schneider, R. (2016). "Porous Mn-doped ZnO nanoparticles for enhanced solar and visible light photocatalysis." *JMADE*, Vol. 101, pp. 309–316.

Ahmed, S. A. (2017). "Structural, optical, and magnetic properties of Mn-doped ZnO samples." *Results Phys*., Vol. 7, pp. 604–610.

Altintas Yildirim, O., Arslan, H. and Sönmezoğlu, S. (2016). "Facile synthesis of cobalt-doped zinc oxide thin films for highly efficient visible light photocatalysts." *Appl. Surf. Sci*., Vol. 390, pp. 111–121.

Alvi, N. H., Hasan, K., Nur, O. and Willander, M. (2011). "The origin of the red emission in n-ZnO nanotubes / p-GaN white light emitting diodes." *Nanoscale Research Lett*., Vol. pp. 1–7.

Anandan, S., Vinu, A., Mori, T., Gokulakrishnan, N., Srinivasu, P., Murugesan, V. and Ariga, K. (2007). "Photocatalytic degradation of 2,4,6-trichlorophenol using lanthanum doped ZnO in aqueous suspension." *Catal. Commun*., Vol. 8, pp. 1377–1382.

Awad, M. A., Ahmed, A. M., Khavrus, V. O. and Ibrahim, E. M. M. (2015). "Tuning the morphology of ZnO nanostructure by in doping and the associated variation in electrical and optical properties." *Ceram. Int*., Vol. 41, No. 8, pp. 10116–10124.

Bahnemann, D. W., Kormann, C. and Hoffmann, M. R. (1987). "Preparation and characterization of quantum size zinc oxide: a detailed spectroscopic study." *J. Phys. Chem*., Vol. 91, No. 14, pp. 3789-3798.

Barzgari, Z., Ghazizadeh, A. and Zahra, S. (2016). "Preparation of Mn-doped ZnO nanostructured for photocatalytic degradation of Orange G under solar light." *Res. Chem. Intermed*., Vol. 42, No. 5, pp. 4303–4315.

Bhatia, S., Verma, N. and Bedi, R. K. (2017). "Sn-doped ZnO nanopetal networks for efficient photocatalytic degradation of dye and gas sensing applications" *Appl. Surf. Sci*., Vol. 407, pp. 495–502.

Chang, Y. Q., Wang, P. W., Ni, S. L., Long, Y. and Li, X. D. (2012). "Influence of Co Content on Raman and Photoluminescence Spectra of Co Doped ZnO Nanowires." *J. Mater. Sci. Technol*., Vol. 28, No. 4, pp. 313–316.

Chauhan, R., Kumar, A. and Chaudhary, R. P. (2012). "Structural and photocatalytic studies of Mn doped TiO2 nanoparticles." *Spectrochim. Acta – Part A Mol. Biomol. Spectrosc*., Vol. 98, pp. 256–264.

Choudhury, S., Sain, S., Mandal, M. K., Pradhan, S. K. and Meikap, A. K. (2016). "Investigation of dielectric and electrical behavior of nanocrystalline Zn1−xMnxO (x = 0 to 0.10) semiconductors synthesized by mechanical alloying." *Physica E*, Vol. 81, pp. 122 130.

Cohn, A.W., Kittilstved, K. R. and Gamelin, D. R. (2012). "Tuning the Potentials of "Extra" Electrons in Colloidal n-Type ZnO Nanocrystals via Mg2+ Substitution." *J. Am. Chem. Soc*., Vol. 134, No. 18, pp. 7937-7943.

Das, S. N. Moon, K. J., Kar, J. P., Choi, J. H., Xiong, J., Lee, T. and Myoung, J. M. (2010). "ZnO single nanowire-based UV detectors." *Appl. Phys. Lett*., Vol. 97, pp. 022103.

Deka, S. and Joy, P. A. (2007). "Synthesis and magnetic properties of Mn doped ZnO nanowires." *Solid State Commun*., Vol. 142, No. 4, pp. 190–194.

Dhara, A., Sain, S., Das, S. and Pradhand, S. K. (2018). "Microstructure, optical, dielectric and electrical characterizations of Mn doped ZnO nanocrystals synthesized by mechanical alloying." *Ceramics International*, Vol. 44, pp. 7110-7121.

Djurisic, A. B., Leung, Y. H., Tam, K. H., Ding, L., Ge, W. K., Chen, H. Y. and Gwo, S. (2006). "Green, yellow, and orange defect emission from ZnO nanostructures: Influence of excitation wavelength." *Applied Physics Letters*, Vol. 88, No. 10, pp. 28–31.

Donkova, B., Dimitrov, D., Kostadinov, M., Mitkova, E. and Mehandjiev, D. (2010). "Catalytic and photocatalytic activity of lightly doped catalysts M:ZnO (M = Cu, Mn)." *Mater. Chem. Phys*., Vol. 123, pp. 563–568.

El Hichou, A., Addou, M., Ebothé, J., Troyon, M. (2005). "Influence of deposition temperature (Ts), air flow rate (f) and precursors on cathodoluminescence properties of ZnO thin films prepared by spray pyrolysis." *J Lumines*, Vol. 113, pp. 183–190.

Emanetoglu, N. W., Gorla, C., Liu, Y., Liang, S. and Lu, Y. (1999). "Epitaxial ZnO piezoelectric thin films for saw filters." *Mater. Sci. Semicond. Process*., Vol. 2, No. 3, pp. 247–252.

Erhart, P., Albe, K. and Klein, A. (2006). "First-principles study of intrinsic point defects in ZnO: Role of band structure, volume relaxation, and finite-size effects." *Physical Review B - Condensed Matter and Materials Physics*, Vol. 73, No. 20, pp. 1–9.

Fabbiyola, S., Sailaja, V., Kennedy, J., Bououdina, L., Judith, M. and Vijaya, J., (2017). "Optical and magnetic properties of Ni-doped ZnO nanoparticles." *Journal of Alloys and Compounds*, Vol. 694, pp. 522-531.

Fan, Z., Wang, D., Chang, P., Tseng, W. and Lu, J. G. (2004). "ZnO nanowire field-effect transistor and oxygen sensing property." *Appl. Phys. Lett*., Vol. 84, pp. 5923.

Gong, Y., Andelman, T., Neumark, G. F., O'Brien, S. and Kuskovsky, I. L. (2007). "Origin of defect-related green emission from ZnO nanoparticles: effect of surface modification." *Nanoscale Res. Lett.*, Vol. 2, pp. 297–302.

Glushenkov, A. M., Zhang, H. Z., Zou, J., Lu, G. Q. and Chen, Y. (2007). "Efficient production of ZnO nanowires by a ball milling and annealing method," *Nanotechnology*, Vol. 18 No. 17, pp. 175604 (6pp).

Janotti, A. and Van De Walle, C. G. (2005). "Oxygen vacancies in ZnO." *Applied Physics Letters*, Vol. 87, No. 12, pp. 1–3.

Kaftelen, H., Ocakoglu, K., Thomann, R., Tu, S., Weber, S. and Erdem, E. (2012). "EPR and photoluminescence spectroscopy studies on the defect structure of ZnO nanocrystals." *Phys. Rev. B*, Vol. 86, No. 1, pp. 1–9.

Kadam, A. N., Kim, T. G., Shin, D. S., Garadkar, K. M. and Park, J. (2017). "Morphological evolution of Cu doped ZnO for enhancement of photocatalytic activity." *J. Alloys Compd*., Vol. 710, pp. 102–113.

Karmakar, R., Neogi, S. K., Banerjee, A. and Bandyopadhyay, S. (2012). "Structural; morphological; optical and magnetic properties of Mn doped ferromagnetic ZnO thin film." *Appl. Surf. Sci*., Vol. 263, pp. 671–677.

Khanna, S. N., Rao, B. K., Jena, P. and Knickelbein, M. (2003). "Ferrimagnetism in Mn 7 cluster." *Chem. Phys. Lett*., Vol. 378, No. 3, pp. 374–379.

Keis, K., Baue, C., Boschloo, G., Hagfeldt, A., Westermark, K., Rensmo, H. and Siegbahn, H. (2002). "Nanostructured ZnO electrodes for dye-sensitized solar cell applications." *J. Photochem. Photobiol. A: Chem*., Vol. 148, pp. 57–64.

Koch, M. H., Timbrell, P. Y. and Lamb, R. N. (1995). "The influence of film crystallinity on the coupling efficiency of ZnO optical modulator waveguides." *Semicond. Sci. Technol*., Vol. 10, pp. 1523–1527.

Law, M., Greene, L. E., Johnson, J. C., Saykally, R. and Yang, P. D. (2005). "Nanowire dye-sensitized solar cells." *Nat. Mater*., Vol. 4, No. 6, pp. 455–459.

Li, W. J., Shi, E. W., Zheng, Y. Q. and Yin, Z. W. (2001). "Hydrothermal preparation of nanometer ZnO nanopowders." *J. Mater. Sci. Lett*., Vol. 20, pp. 1381-1383.

Ma, Q., Lv, X., Wang, Y. and Chen, J. (2016). "Optical and photocatalytic properties of Mn doped flower-like ZnO hierarchical structures." *Opt. Mater*., Vol. 60, pp. 86–93.

Martinson, A. B. F., Elam, J. W., Hupp, J. T. and Pellin, M. J. (2007). "ZnO Nanotube Based Dye-Sensitized Solar Cells." *Nano Lett*., Vol. 7, No. 8, pp. 2183–2187.

Mei, Y. F., Siu, G. G., Fu, R. K. Y., Wong, K. W., Chu, P. K., Lai, C. W. and Ong, H. C. (2005). "Determination of nitrogen-related defects in N-implanted ZnO films by dynamic cathodoluminescence." *Nuclear Instruments and Methods in Physics Research, Section B: Beam Interactions with Materials and Atoms*, Vol. 237, pp. 307–311.

Moontragoon, P., Pinitsoontorn, S. and Thongbai, P. (2013). "Mn-doped ZnO nanoparticles: Preparation, characterization, and calculation of electronic and magnetic properties." *Microelectron. Eng*., Vol. 108, No. 3, pp. 158–162.

Motaung, D. E., Kortidis, I., Papadaki, D., Nkosi, S. S., Mhlongo, G. H., Wesley-Smith, J., Malgas, G. F., Mwakikunga, B. W., Coetsee, E., Swart, H. C., Kiriakidis, G. and Ray, S. S. (2014). "Defect-induced magnetism in un-doped and Mn-doped wide band gap Zinc oxide grown by aerosol spray pyrolysis." *Appl. Surf. Sci*., Vol. 311, pp. 14-26.

Nasser, R., Othmen, W. B. H., Elhouichet, H. and Férid, M. (2017). "Preparation, characterization of Sb-doped ZnO nanocrystals and their excellent solar light driven photocatalytic activity." *Appl. Surf. Sci*., Vol. 393, pp. 486–495.

Othman, A. A., Osman, M. A., Ibrahim, E. M. M., Ali, M. A. and Abd-Elrahim, A. G. (2017). "Mn-doped ZnO nanocrystals synthesized by sonochemical method: Structural, photoluminescence, and magnetic properties." *Materials Science and Engineering: B*, Vol. 219, pp. 1-9.

Putri, N. A., Fauzia, V., Iwan, S., Roza, L., Umar, A. A.

and Budi, S. (2018). "Mn-doping-induced photocatalytic activity enhancement of ZnO nanorods prepared on glass substrates." *Applied Surface Science*, Vol. 439, pp. 285–297.

Radoi, R., Fern ndez, P., Piqueras, J., Wiggins, M. S. and Solis, J. (2003). "Luminescence properties of mechanically milled and laser irradiated ZnO." *Nanotechnology*, Vol. 14, pp. 794–798.

Saito, N., Haneda, H., Sekiguchi, T., Ohashi, N., Sakaguchi, I. and Koumoto, K. (2002). " Low ‐ Temperature Fabrication of Light ‐ Emitting Zinc Oxide Micropatterns Using Self ‐ Assembled Monolayers." *Adv. Mater*., Vol. 14, No. 6, pp. 418-421.

Saleh, R. and Djaja, N. F. (2014). "Transition metal-doped ZnO nanoparticles: Synthesis, characterization and photocatalytic activity under UV light." *Spectrochim. Acta – Part A Mol. Biomol. Spectrosc*., Vol. 130, pp. 581–590.

Samanta, A., Goswami, M. N. and Mahapatra, P. K. (2018). "Magnetic and electric properties of Ni-doped ZnO nanoparticles exhibit diluted magnetic semiconductor in nature." *Journal of Alloys and Compounds*, Vol. 730, No. 399–407.

Schneider, J. J., Hoffmann, R. C., Engstler, J., Klyszcz, A., Erdem, E., Jakes, P., Eichel, R. A., Pitta-Bauermann, L. and Bill, J. (2010). "Synthesis, characterization, defect chemistry, and FET properties of microwave-derived nanoscaled zinc oxide." *Chem. Mater*., Vol. 22, No. 2203-2212.

Sekine, N., Chou, C. H., Kwan, W. L. and Yang, Y. (2009). "ZnO nano-ridge structure and its application in inverted polymer solar cell." *Org. Electron*, Vol. 10, No. 8, pp. 1473–1477.

Studenikin, S. A., Golego, N. and Cocivera, M. (1998). "Fabrication of green and orange photoluminescent, undoped ZnO films using spray pyrolysis." *Journal of Applied Physics*, Vol. 84, No. 4, pp. 2287–2294.

Tabib, A., Bouslama, W., Sieber, B., Addad, A., Elhouichet, H., Férid, M. and Boukherroub, R. (2017). "Structural and optical properties of Na doped ZnO nanocrystals: application to solar photocatalysis." *Appl. Surf. Sci*., Vol. 396, pp. 1528–1538.

Toloman, D., Mesaros, A., Popa, A., Raita, O., Silipas, T. D., Vasile, B. S., Pana, O. and Giurgiu, L. M. (2013). "Evidence by EPR of ferromagnetic phase in Mn-doped ZnO nanoparticles annealed at different temperatures." *Journal of Alloys and Compounds*, Vol. 551, pp. 502-507.

Ullah, R. and Dutta, J. (2008). "Photocatalytic degradation of organic dyes with manganese doped ZnO nanoparticles." *J. Hazard. Mater*., Vol. 156, pp. 194–200.

Umar, K., Aris, A., Parveen, T., Jaafar, J., Abdul Majid, Z., Vijaya Bhaskar Reddy, A. and Talib, J. (2015). "Synthesis, characterization of Mo and Mn doped ZnO and their photocatalytic activity for the decolorization of two different chromophoric dyes." *Appl. Catal. A Gen*., Vol. 505, pp. 507–514.

Vijayalakshmi, K. and Sivaraj, D. (2015). "Enhanced antibacterial activity of Cr doped ZnO nanorods synthesized using microwave processing." *RSC Adv*., Vol. 5, pp. 68461–68469.

Vlasenko, L. S. and Watkins, G. D. (2005). "Optical detection of electron paramagnetic resonance for intrinsic defects produced in ZnO by 2.5-MeV electron irradiation in situ at 4.2 K." *Physical Review B - Condensed Matter and Materials Physics*, Vol. 72, No. 3, pp. 1–12.

Wang, J., Yang, J., Han, N., Zhou, X., Gong, S., Yang, J., Hu, P. and Chen, Y. (2017). "Highly sensitive and selective ethanol and acetone gas sensors based on modified ZnO nanomaterials." *Materials and Design*, Vol. 121, pp. 69–76.

Wang, J., Yang, P. and Wei, X. (2015). "High-Performance, Room-Temperature, and No-Humidity-Impact Ammonia Sensor Based on Heterogeneous Nickel Oxide and Zinc Oxide Nanocrystals." *ACS Appl. Mater*. Interfaces, Vol. 7, No. 6, pp. 3816–3824.

Wang, N., Yang, Y. and Yang, G. (2011). "Great blue-shift of luminescence of ZnO nanoparticle array constructed from ZnO quantum dots." *Nanoscale Res. Lett.*, Vol. 338, pp. 6.

Wei, S., Lian, J. and Wu, H. (2010). "Annealing effect on the photoluminescence properties of ZnO nanorod array prepared by a PLD-assistant wet chemical method." *Mater. Charact*., Vol. 61, No. 11, pp. 1239–1244.

Wu, L., Wu, Y., Pan, X. and Kong, F. (2006). "Synthesis of ZnO nanorod and the annealing effect on its photoluminescence property." *Opt Mater*., Vol. 28, pp. 418–422.

Yang, J., Li, X., Lang, J., Yang, L., Gao, M., Liu, X., Wei, M., Liu, Y. and Wang, R. (2011). "Effects of mineralizing agent on the morphologies and photoluminescence properties of Eu3+-doped ZnO nanomaterials." *J. Alloys Compd*., Vol. 509, No. 41, pp. 10025–10031.

Yildirimcan, S., Ocakoglu, K., Erat, S., Emen, F. M., Repp, S. and Erdem, E. (2016). "The effect of growing time and Mn concentration on the defect structure of ZnO nanocrystals: X-ray diffraction, infrared and EPR spectroscopy." *RSC Adv*., Vol. 6, No. 45, pp. 39511–39521.